

Electrochemical methods are versatile and powerful analytical techniques that offer high sensitivity – An overview

***B.Mehaboob Basha,**

Lecturer in Chemistry, Shri Sangameshwar Arts, Commerce and Science P U College, Chadchan.

Abstract:

In this paper author seeks to present electrochemical methods and its significance. Aminoantipyrin is an aromatic substance with analgesic, antipyretic and anti-inflammatory properties. However, AAP usually produces side effects such as the risk of agranulocytosis. Although AAP is scarcely ever administered as an analgesic because of side effects, as a raw material, it is mostly used to produce 4-aminoantipyrine derivatives, which have better biological activities. In addition, it is used as a reagent for biochemical reactions producing peroxides or phenols and can also be used to detect phenols in the environment. Since it is widely used in the pharmaceutical industry, biochemical research and environmental monitoring, AAP has become an environmental pollutant. The toxic effect of AAP on experimental animals was reported. AAP can reduce blood flow, and 13,14-dihydro-15-keto prostaglandin F₂ alpha concentration after it is infused into the blood. AAP can form stable complexes with heme. Different methods have been reported for the determination of AAP including liquid and gas chromatography, spectrophotometric method, liquid chromatography/mass spectrometry, capillary electrophoresis, solid phase spectrophotometry, different HPLC methods and voltammetric method by using graphite pencil electrode. The main problems encountered in using some methods are time-consuming extraction and separation procedure and high cost.

Keywords: Electrochemical, methods, versatile, powerful, analytical techniques, offer high, sensitivity, precision.

Introduction:

To the best of our knowledge, there are no reports based on graphene modified glassy carbon electrode for the determination of AAP. Hence, we have undertaken the development of electrochemical method for the determination of AAP at graphene modified electrode in this discussion.

EXPERIMENTAL Materials and Reagents

The powdered form of 4-Aminoantipyrine (AAP) was obtained from Sigma Aldrich and used without further purification. A stock solution (1.0 mM) of AAP was prepared in double distilled water. The phosphate buffers from pH 3.0 – 9.2 were prepared in double distilled water as described by Christian and Purdy³⁷. All chemicals used were of reagent grade and double distilled water was used throughout the work. A solution of AAP was prepared by dissolving an appropriate amount of recrystallised sample in double distilled water. The required concentration of AAP was used from its aqueous solution.

Instrumentation

Electrochemical measurements were carried out on a CHI 630D electrochemical analyzer (CH Instruments Inc., USA). The voltammetric measurements were carried out in a 10 ml single compartment three-electrode glass cell with Ag/AgCl as a reference electrode, a platinum wire as counter electrode and GPN

modified with GCE (GPN/GCE) as a working electrode. All the potentials are given against the Ag/AgCl (3 M KCl). All experiments were carried out at an ambient temperature of $25^{\circ}\text{C} \pm 0.1^{\circ}\text{C}$. The pH measurements were performed with Elico LI120 pH meter (Elico Ltd., India).

At different scan rates, the area of the electrode was calculated using 1.0 mM $\text{K}_3[\text{Fe}(\text{CN})_6]$ as a probe. For a reversible process, the Randles-Sevcik formula has been used³⁸.

$$i_{\text{pa}} = (2.69 \times 10^5) n^{3/2} A D_0^{1/2} C_0 \nu^{1/2} \quad (1)$$

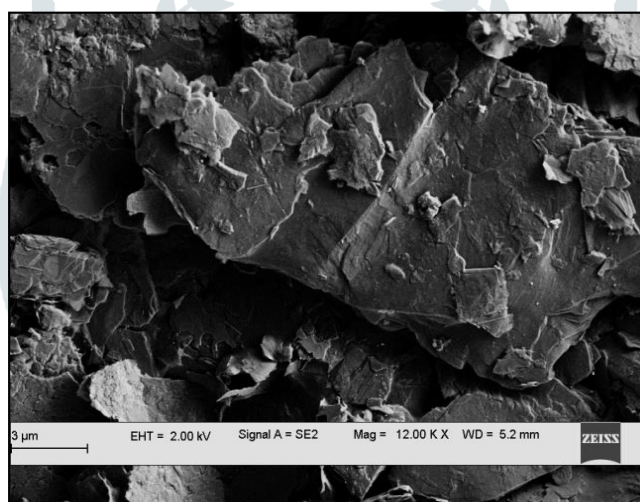
where, i_{pa} refers to the anodic peak current, n is the number of electrons transferred, A is the surface area of the electrode, D_0 is diffusion coefficient, ν is the scan rate and C_0 is the concentration of $\text{K}_3[\text{Fe}(\text{CN})_6]$. For 1.0 mM $\text{K}_3[\text{Fe}(\text{CN})_6]$ in 0.1 M KCl electrolyte, $n = 1$, $D_0 = 7.6 \times 10^{-6} \text{ cm}^2 \text{ s}^{-1}$, then from the slope of the plot of i_{pa} versus $\nu^{1/2}$ relation, the surface area of electrodes were calculated and found to be 0.0462 cm^2 for GCE and 0.295 cm^2 for GPN/GCE.

Synthesis of GPN

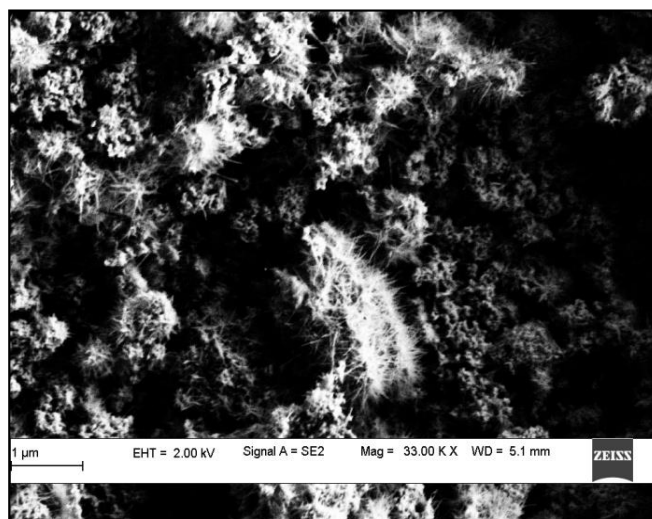
Graphene oxide (GO) was synthesized from natural graphite powder by the Hummer's method.³⁹ In brief, natural graphite powder was treated with concentrated sulfuric acid and hydrochloric acid with potassium permanganate for 96 hours. After complete oxidation of graphite, the oxidized mixture was added to excess water, washed with 5% HCl and repeatedly treated with water to obtain neutral graphite oxide. Then through extreme heating and continuous splitting of graphite oxide, fabric graphene sheets were obtained.

Figure 1

(a) SEM images of the surface of graphite powder



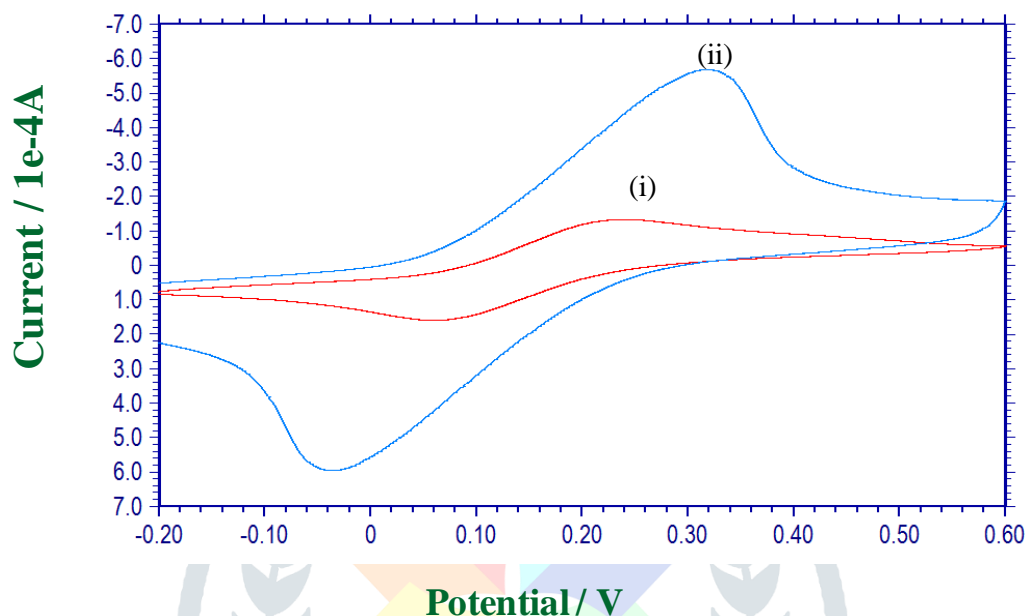
(b) SEM images of the surface of graphene powder



Electrochemical investigation of potassium ferricyanide at graphene modified GCE

Potassium ferricyanide $K_3[Fe(CN)_6]$ was used as the electrochemical redox probe to investigate the electrochemical properties of GPN/GCE (Figure 2). The cyclic voltammograms (CVs) of GPN/GCE showed that the redox peak current increased compared to bare GCE. At the bare GCE the cyclic voltammogram of $K_3[Fe(CN)_6]$ (Curve i) showed a pair of redox peaks with the anodic peak potential at 221 mV and the cathodic peak potential at 65.9 mV in 0.1M KCl. The GPN/GCE shows a pair of redox peaks (curve ii). The anodic peak potential was located at 316.8 mV and the cathodic peak potential at 43.3 mV respectively. The results of the enhancement of peak current showed excellent catalytic activity of GPN/GCE

Figure 2 Cyclic voltammograms obtained for 1.0 mM $K_3 [Fe(CN)_6]$ solution at scan rate of 100 mV s^{-1} for (i) GCE and (ii) GPN/GCE.

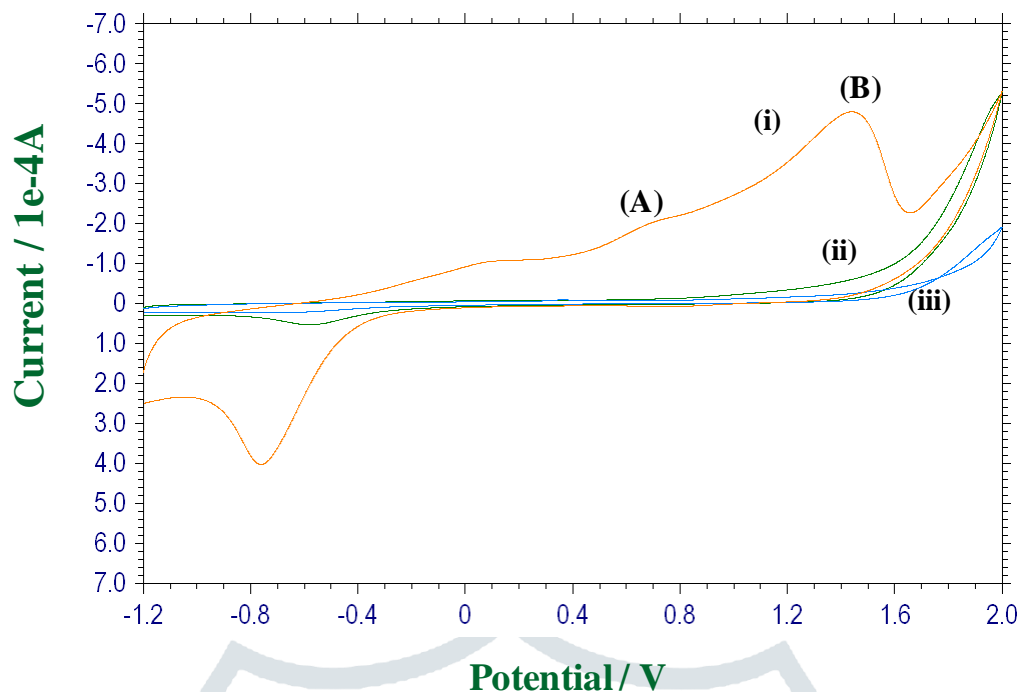


Electrochemical behavior of AAP on GPN/GCE

Figure 3 displayed the cyclic voltammograms of 1mM AAP at GPN/GCE (curve i) and GCE (curve iii) in 0.2 M (pH 3.0), respectively. The curve (ii) in Figure 3 was blank voltammograms of GPN/GCE showing one reduction peak. The voltammogram obtained for AAP at GCE (curve i) shows no redox peaks. However, in the case of GPN/GCE (Figure 3), two oxidation peaks and one reduction peak which was also observed in the absence of AAP, were observed. So, only oxidation peaks can be assigned to AAP. The peak (B) has better shape as compared to peak (A). Hence, the peak (B) was considered for the analysis. The significantly enhanced voltammetric response of AAP on GPN/GCE could be reasonably ascribed to the large specific surface area and electrocatalytic activity of GPN film.

For further investigating the redox properties of AAP at the GPN/GCE, successive cyclic scan was performed in a 1mM AAP solution. It could be seen that the anodic peak current decreased obviously in the second scan compared with that of the first one, and gradually reduced with successive cyclic sweep. The reason may be that the oxidation product of AAP, adhered to the electrode surface and hindered the access of AAP. Accordingly, the first cyclic sweep was adopted.

Figure 3 Cyclic voltammograms obtained in pH 3.0, 0.2 M phosphate buffer at scan rate of 50 mVs^{-1} for (i) GPN/GCE with AAP, (ii) GPN/GCE without AAP, and (iii) GCE with AAP.



Influence of pH

The effect of solution pH on the voltammetric response of AAP (1mM) was investigated in pH range from 3.0 to 9.2 as shown in Figure 4 (a). As increasing the pH, the peak potential of AAP shifted negatively from 1.53 to 1.51 V as shown in Figure 4(b). The shift in E_p with pH refers to a proton transfer in the electrochemical oxidation of AAP.

The potential diagram was constructed by plotting the graph of peak B potentials, E_p versus pH of the buffer with good linearity (Figure 4 (c)). The slope obtained was 58.9 mV/pH (equation 1); it reveals that the number electrons and protons involved in the reaction are equal.⁴⁰ From the Figure 4 (b), it was clear that the peak current was high for the 1.0 mM AAP in the supporting medium at pH 3. Therefore, for further determination of AAP, the pH 7 was selected as the optimum pH value.

$$\log I_{pa}(A) = -0.0581 \text{ pH} + 1.22; (r = 0.6813) \quad (1)$$

Figure 4(a) Cyclic voltammograms obtained for 1.0 mM AAP at GPN/GCE with potential scan rate 50 mVs⁻¹ in phosphate buffer solution of pH (i) 3.0, (ii) 4.0, (iii) 5.0, (iv) 7.0, (v) 8.0, and (vi) 9.2

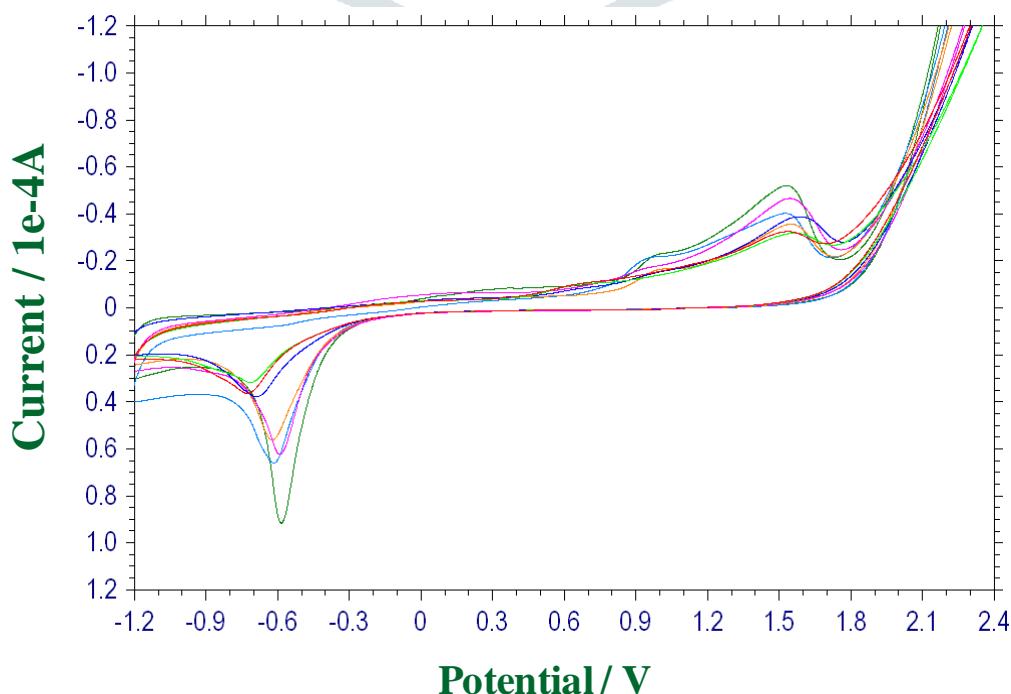
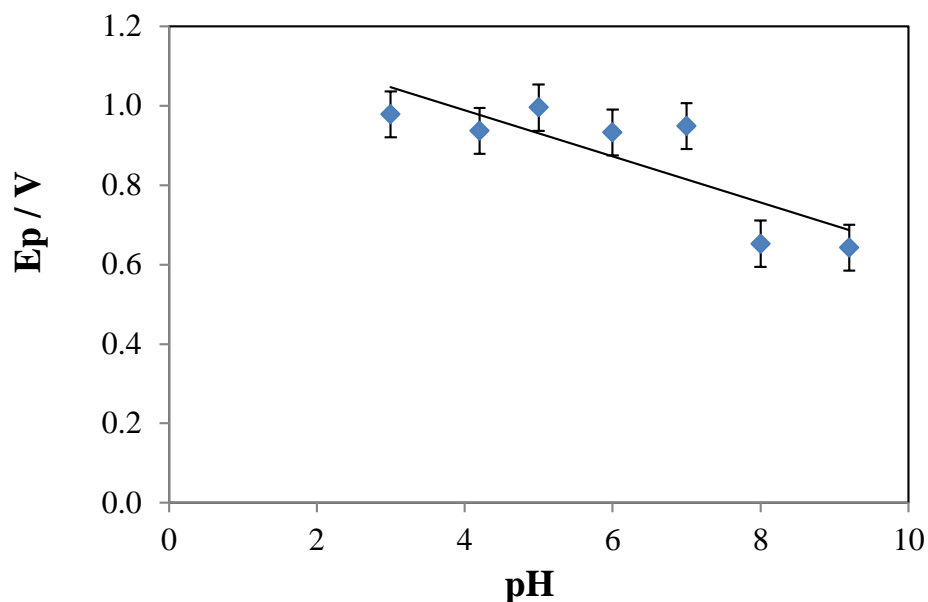
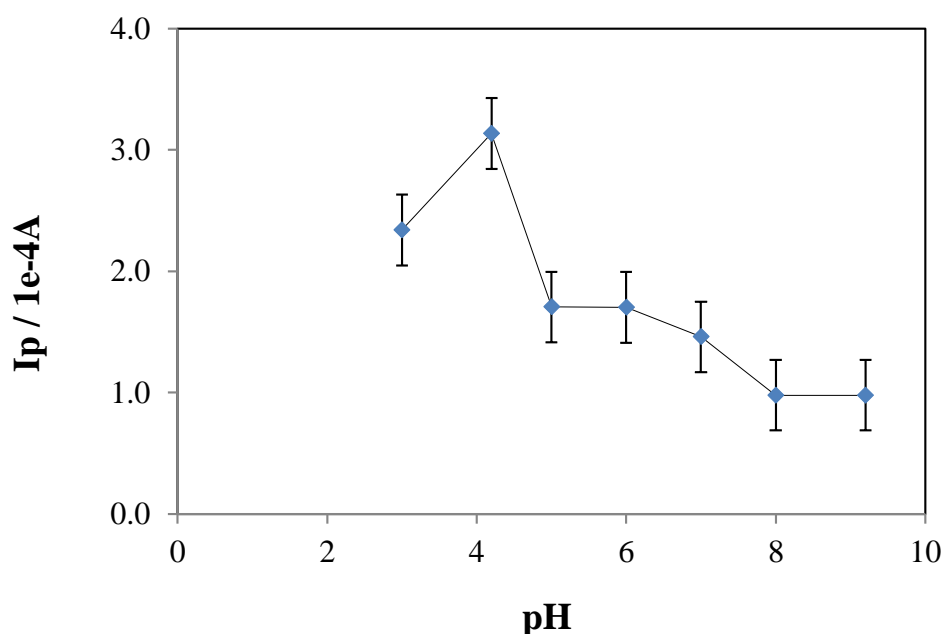


Figure 4 (b) Variation of peak potential with pH for 1.0 mM AAP.**(c)** Variation of peak current with pH for 1.0 mM AAP

Effect of scan rate

The influence of scan rate plays an important role in voltammetric oxidation reactions. So, it is important to evaluate the dependence of peak current and peak potential on the scan rate and whether the electrode reaction was adsorption or diffusion controlled process. GPN/GCE showed increase in the redox peak currents with increase in the scan rate from 25 to 275 mV/s in 0.20 M phosphate buffer solution as shown in Figure 5 (a).

A good linearity was observed between logarithm of peak B current and logarithm of scan rate as shown in Figure 5(b) with slope value 0.37 indicating the electrode reaction was purely diffusion controlled⁴¹ and the linear equation is as follows.

$$\log I_{pa}(A) = 0.3692 \log v (Vs^{-1}) + 0.0363; (r = 0.874) \quad (2)$$

Laviron equation⁴² (equation 3) has been employed to find out the number of electrons transferred (n) and heterogeneous rate constant (k^0) for an irreversible electrode reaction.

$$E_p = E^0 + \left(\frac{2.303RT}{\alpha nF} \right) \log \left(\frac{RTk^0}{\alpha nF} \right) + \left(\frac{2.303RT}{\alpha nF} \right) \log \nu \quad (3)$$

where, α is the transfer coefficient, ν the scan rate and E^0 is the formal standard redox potential. Other symbols have their usual meaning. The αn was calculated by using the slope of plot of E_p versus $\log \nu$ (equation 4, Figure 5 (c)),

$$E_p \text{ (V)} = 0.136 \log \nu \text{ (Vs}^{-1}\text{)} + 1.319; (r = 0.9718) \quad (4)$$

Bard and Faulkner formula⁴³ (equation 5) was used to evaluate the value of α .

$$\alpha = \frac{47.7}{E_p - E^0} \text{ mV} \quad (5)$$

The values of αn and α were found to be 20.43 and 0.1. So, the number of electrons (n) transferred in electro-oxidation of AAP was calculated to be 4.3 ~ 4. The heterogeneous rate constant, k^0 can be evaluated if the value of E^0 is known. The value of E^0 found to be 1.51 which was intercept of plot of E_p versus ν extrapolated at $\nu = 0$. Thus, the value of k^0 was found to be $5.7 \times 10^1 \text{ s}^{-1}$.

Figure 5(a) Cyclic voltammograms obtained for 1.0 mM AAP at GPN/GCE in phosphate buffer solution of pH 3.0 at scan rates of (i) 25, (ii) 75, (iii) 125, (iv) 175, (v) 225, and (vi) 275 mVs^{-1}

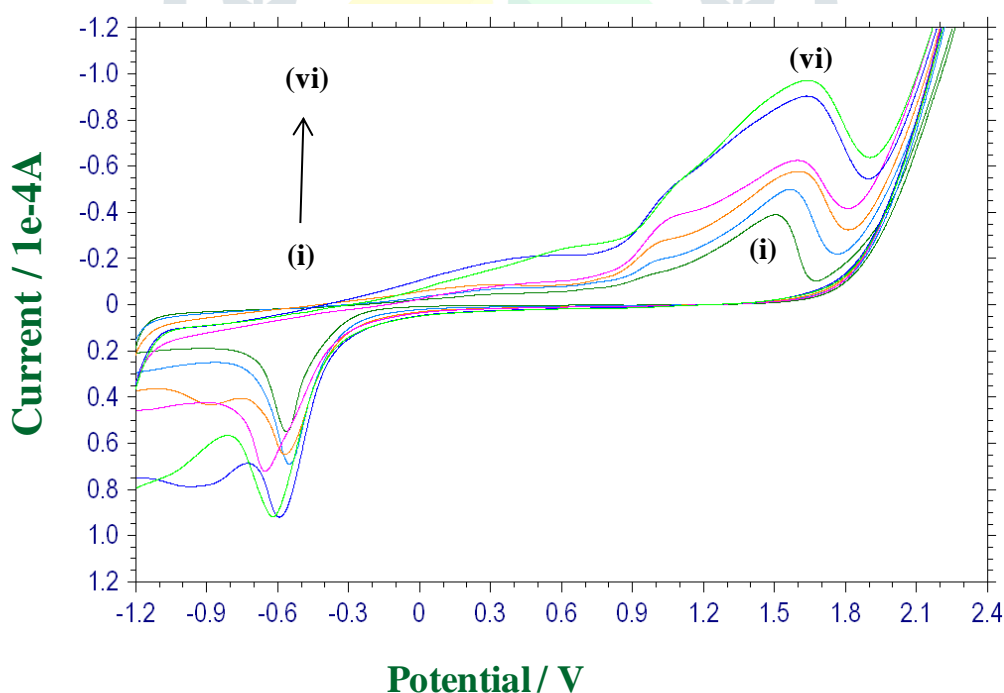
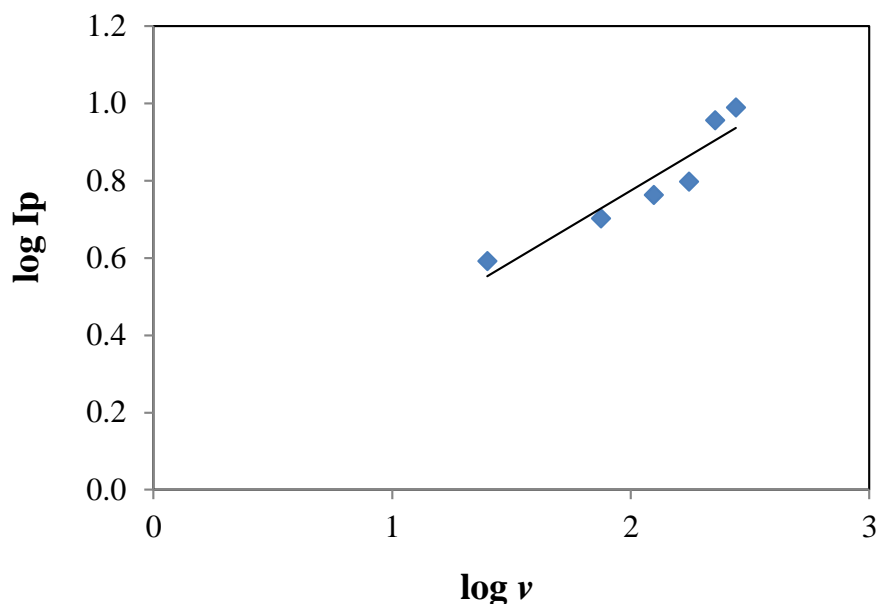
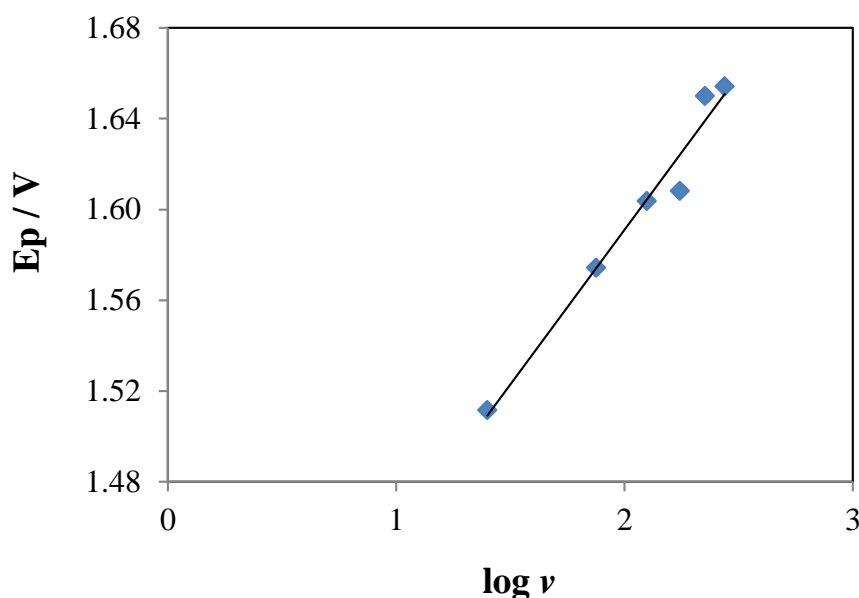


Figure 5 (b) Linear relationship between the log I_p and log ν for peak B**Figure 5 (c)** Linear relationship between the peak potential and logarithmic scan rate for peak B

Analytical applications

The linear sweep voltammetry (LSV) technique was applied to the determination of AAP since, it produced peak current with much more intense than that produced by cyclic voltammetry (CV). In order to estimate the sensor's detection limit, selectivity and sensitivity a calibration curve of the dependence of peak current on analyte's concentration was established in the larger concentration range (Figure 6 (a)). There was a linear relationship between peak current and [AAP] over the concentration range from 1 – 15 nM (Figure 6 (b)) with correlation coefficient 0.9612 and corresponding linear equation is

$$I_p(10^{-4}A) = 0.1195[AAP](nM) + 2.868 ; R^2 = 0.9612 \quad (6)$$

The limit of detection (LOD) and limit of quantification (LOQ) were calculated using the equation (7).

$$LOD = 3s/m \quad LOQ = 10s/m \quad (7)$$

where s is the standard deviation of the peak current of (five runs) of the lowest concentration of the linearity range (1.0 nM) and m is the slope of the calibration curve.⁴⁴ Therefore, the values of LOD and LOQ were found to be 0.52 nM and 1.75 nM respectively. The detection limits of earlier reports⁴⁵⁻⁴⁹ were listed in the Table 1. So, it was clear that the present method proposes lower LOD and LOQ values compared to previous reports in the literature.

Conclusions

The results of the present work demonstrated that GPN/GCE exhibit electrocatalytic effect on AAP oxidation. In comparison with the bare a GPN/GCE, the resulting GPN/GCE showed better performance, such as obvious enhanced peak potential and peak background current. The GPN/GCE was then used for the determination of AAP in a linear range of 1 nM – 15 nM with detection limit of 0.52 nM. The GPN/GCE possessed high selectivity, sensitivity, stability and a low detection limit, which makes it suitable for facilitating the electrocatalytic activity for the oxidation of AAP determination. Moreover, the GPN/GCE was also applied for the determination of AAP in urine samples with satisfactory results making it practical for routine analysis. The proposed method is suitable for quality control laboratories as well as pharmacokinetic studies where economy and time are essential.

REFERENCES

1. S. Giljie, S. Han, M. S. Wang, K. L. Wang and R. B. Kaner, *Nano Lett.*, **7**, 3394 (2007)
2. E. Yoo, J. Kim, E. Hosono, H.S. Zhou, T. Kudo and I. Honma, *Nano Lett.*, **8**, 2277 (2008)
3. P. K. Aneesh, S. R. Nambiar, T. P. Rao and A. Ajayaghosh, *Anal. Methods*, **6**, 5322 (2014)
4. L. Chen, Y. Tang, K. Wang, C. Liu and S. Luo, *Electrochem. Commun.*, **13**, 133 (2011)
5. S. M. Patil, S. R. Sataraddi, A. M. Bagoji, R. M. Pathan and S. T. Nandibewoor, *Electroanalysis*, **26**, 831 (2014)
6. L. C. S. Figueiredo-Filho, D. A. C. Brownson, O. Fatibello-Filho and C. E. Banks, *Analyst*, **138**, 4436 (2013)
7. Y.M. Chen and Y.P. Chen, *Fluid Phase Equilib.* **282**, 82 (2009)
8. A. Lang, C. Hatscher and Wiegert, et *Amino Acids*, **36**, 333 (2009)
9. S. Cunha, S.M. Oliveira and M.T. Rodrigues *J. Mol. Struct.*, **752**, 32 (2005)
10. S. Prasad and R.K. Agarwal *Transit. Met. Chem.* **32**, 143 (2007)
11. J.F. Van Staden, N.W. Beyene and R.I. Stefan *Talanta*, **68**, 401 (2005)
12. J. Kasthuri, J. Santhanalakshmi and N. Rajendiran *Transit. Met. Chem.*, **33**, 899 (2008)
13. C. Z. Katsaounos, E. K. Paleologos, D.L. Giokas and M. I. Karayannis *Int. J. Environ. Anal. Chem.*, **83**, 507 (2003)
14. A.M. Vinagre, E.F. Collares, *Braz. J. Med. Biol. Res.*, **40**, 903 (2007)
15. S.G. Sunderji, A. El Badry, E.R. Poore, et al., *Am. J. Obstet. Gynecol.* **149**, 408 (1984)
16. A. El Badry, J. P. Figueroa, E. R. Poore, et al., *Am. J. Obstet. Gynecol.*, **150**, 474 (1984)
17. S. C. Pierre, R. Schmidt, C. Brenneis, et al., *Br. J. Pharmacol.*, **151**, 494 (2007)